Dynamical stability of the Gliese 581 exoplanetary system

Zs. Tóth[1,★] and **I. Nagy**[2,3]

[1] Department of Geosciences, University of Bremen, Klagenfurter Straße, 23359 Bremen, Germany
[2] Department of Natural Science, National University of Public Service, Hungária körút 9-11, 1101 Budapest, Hungary
[3] Department of Astronomy, Eötvös Loránd University, Pázmány Péter sétány 1/A, 1117 Budapest, Hungary

Using numerical methods we investigate the dynamical stability of the Gliese 581 exoplanetary system. The system is known to harbour four certain planets (b-e). The existence of another planet (g) in the liquid water habitable zone of the star is supported by the latest analysis of the radial velocity (RV) measurements. Vogt et al. (AN 333, 561-575, 2012) announced a 4- and a 5-planet model fitted to the RV curve with forced circular orbits. To characterize stability, we used the maximum eccentricity the planets reached over the time of the integrations and the Lyapunov Characteristic Indicator to identify chaotic motion. The integration of the 4-planet model shows that it is stable for even an inclination $i = 5°$, i. e. high planetary masses, on a longer timescale. We varied the orbital parameters of the innermost low-mass planet e, which quickly became unstable in earlier eccentric models. Planet e remained stable during the integration time, although the stable region around its initial semi-major axis and eccentricity is rather small. In the 4-planet model, we looked for stable regions for a fifth planetary body. We found extensive stable regions between the two super-Earth sized planets c and d, and beyond planet d. The Titius-Bode law and its revised version, Ragnarsson's formula applied to the Gliese 581 planetary system both predict distances of additional planets in these stable regions. The planet Gliese 581 g would have a dynamically stable orbit, even for a wider range of orbital parameters. Since circular orbits in the models seem to be a too strong restriction and the true orbits might be elliptic, we investigated the stability of the planets as a function of their eccentricity, and derived dynamical constraints for the ellipticity of the orbits.

1 Introduction

Based on high-precision radial velocity (RV) measurements acquired using the HARPS (Bonfils et al. 2005; Mayor et al. 2009; Udry et al. 2007) and HIRES (Vogt et al. 2010) spectrographs, an exoplanetary system was discovered around the red dwarf star Gliese 581 recently. The RV data suggest that the system harbours at least four, and maybe five or six planets: Gliese 581 e, b, c and d are certain, while the existence of f and g are disputed (Forveille et al. 2011; Vogt et al. 2012).

The planetary system of Gliese 581 consists of a Neptune-mass planet on a 5.36-day orbit (planet b), two super-Earth sized planets (planet c and d) with orbital periods of 12.9 and 67 days, and a low-mass planet closest to the star with an orbital period of 3.15 days, all discovered in the HARPS data sets by Bonfils et al. (2005); Mayor et al. (2009); Udry et al. (2007), respectively. The super-Earth planets in the system are located on the two edges of the liquid water habitable zone, and while the greenhouse effect of the atmosphere would make planet c too warm and therefore unable to host liquid water, high concentrations of carbon dioxide or other greenhouse gases would be suffi-

cient to keep planet d from freezing out at the cold edge of the habitable zone (Selsis et al. 2007).

Combining the 4.3-year HARPS set with the 11-year set of HIRES RVs, Vogt et al. (2010) announced the discovery of planet f and g orbiting the star with periods of 433 and 36.6 days. Both planet f and g were indicated in the combined RV data sets using a Keplerian fit with (forced) circular orbits. The quality of the fit could be improved only when the eccentricities on the 67-day and 36.6-day planets' orbits were allowed to float, with these two planets being in secular resonance. Gliese 581 g with a mass of $\sim 3M_\oplus$ would be a rocky planet in the middle of the habitable zone of the system and might be habitable for a wider range of atmospheric conditions.

Bayesian re-analysis of both the combined and individual datasets by Gregory (2011) and Tuomi (2011) confirmed only four clear planetary signals (planet e, b, c and d) and higher probability for the existence of planet f (with an orbital period of ~ 400 days). Both studies found that the eccentricities for 3 of the 4 orbits are consistent with zero, the orbit of planet d is elliptical ($e_d \simeq 0.4$), similarly to the earlier 4-planet solution of Mayor et al. (2009).

Anglada-Escude et al. (2010) noted how solutions fitting RV data sets with a single-planet eccentric orbit can hide two planets in circular resonant orbits. This is because there is a degeneracy between the resonant and ec-

★ Corresponding author: e-mail: zsuzsanna.toth@gmail.com

centric solutions, as their Keplerian motion equations are identical up to the first order in the eccentricity. In a subsequent study, Anglada-Escude & Dawson (2010) showed that the first eccentricity harmonic of Gliese 581 d (~ 33.5 days) coincides with a yearly alias of the newly reported planet g (~ 33.2 days), thus the high eccentricity of planet d can partially absorb the signal from planet g. Nevertheless, based on statistical tests they concluded that the presence of planet g is well supported by the available RV data. Tadeu dos Santos et al. (2012) similarly concluded that the existence of the 36-day planet g depends on the eccentricity of the 67-day planet d and its detection requires the assumption that all planets are on circular orbits. The signal of planet f was found, but only in the threshold of their confidence level with a period of ~ 455 days.

Forveille et al. (2011) released an additional set of HARPS RV measurements and analysed the then total 7-year data set. Their 4-planet Keplerian-fits, with either fixed or freely floating eccentricities, revealed no significant residual signals, therefore no support for the two additional planets. The additional measurements revised the mass of planet d down to 6 $M_\oplus$, making a rocky composition more likely. Vogt et al. (2012) then re-analyzed this data set and warned that allowing the eccentricities to float, and in particular the eccentricity of planet e to rise, leads to instability and therefore to highly unphysical Keplerian models. None of the N-body simulations of the eccentric Keplerian fit of Forveille et al. (2011) remained dynamically stable on longer time scales due to high eccentricity of planet e. The new 4-planet all-circular interacting model of Vogt et al. (2012) remains dynamically stable for 20 Myrs. Furthermore, it offers confirmative support for a fifth planetary signal near 32-33 days, which could be planet g at its 36-day yearly alias period.

Here we will present a numerical investigation into the dynamical stability of the Gliese 581 system, starting from the 4 and 5-planet models of Vogt et al. (2012). The objective of our study is to set dynamical constraints on the orbits of the latest RV fit, including planet g. Out of curiosity, we test how well the Titius-Bode law describes the Gliese 581 planetary system and where it predicts additional planetary orbits.

2 Titius-Bode law

The Titius-Bode law (TBL) is an empirical formula describing the planetary distances in the Solar System in the form of a power law. Historically, TBL described the planetary orbits from Mercury through Saturn, and correctly predicted the orbits of Ceres and Uranus, but failed when Neptune and the Kuiper Belt objects were discovered. Although no simple physically relevant explanation of the TBL has been found so far, astrophysical studies point to physical background (see the summary of Cuntz 2012), and there has been attempts to investigate if exoplanetary systems fit Titius-Bode like laws, and to use them to predict yet undis-

Table 1 Distances of the planets in the Gliese 581 planetary system based on the Titius-Bode law and the formula of Ragnarsson (1995).

Planet	a (AU)	a_{TBL}	(AU)	a_{RF}	(AU)
e	0.03	$n = -\infty$	0.03	$m = -1$	0.022
b	0.04	$n = 0$	0.04	$m = 0$	0.04
$?$		$n = 1$	0.05		
c	0.07	$n = 2$	0.07	$m = 1$	0.074
g	0.13	$n = 3$	0.11	$m = 2$	0.148
d	0.22	$n = 4$	0.19	$m = 3$	0.221
$?$				$m = 4$	0.294
$?$		$n = 5$	0.35	$m = 5$	0.368

covered exoplanets, e.g. in the 5-planet system of 55 Cancri (Cuntz 2012; Poveda & Lara 2008).

Based on the hypothesis of a geometrical planetary sequence, we calculated the planetary distances in the Gliese 581 system. Using the TBL and a revised formula by Ragnarsson (1995), both adjusted to the known exoplanets of Gliese 581, we search for gaps for additional planets in the inner part of the system (> 0.4 AU).

TBL states that the semi-major axis of the planets are given, in astronomical units, by the formula $a_n = 0.4 + 0.3 \cdot 2^n$, $n = -\infty, 0, 1, 2, \ldots$ Adjusted to the Gliese 581 planetary system it can be written:

$$a_n = 0.03 + 0.01 \cdot 2^n, \ n = -\infty, 0, 1, 2, \ldots \quad (1)$$

Ragnarsson's new empirical formula (RF) is more accurate in describing the Solar System, and is based on the symmetry in the logarithms of the semi-major axes around Jupiter. Assuming that the hot Neptune (planet b) in the Gliese 581 system plays the same dominating role as Jupiter in our Solar System, RF can be written:

$$a_m = a_b \left[(5/2)^{2/3} |m| \right]^{sign(m)}, \ m = -1, 0, 1, \ldots \quad (2)$$

where a_b is the semi-major axis of Gliese 581b, parameter m is the "jovicentric" planet number, which is negative for the inner planets (in this case for planet e).

The distances of the planets calculated from Eq.(1) and Eq.(2) are listed in Table 1. Neither of these formulas seem to describe perfectly the actual values, although both work for three out of the four planets relatively well, in fact it is remarkable how well RF fits for planet c and d. The TBL predicts three more possible planets in the system, but we question if at 0.05 AU, very close to the most massive planet, another stable orbit can exist. Between planet c and d, another planetary body is indicated at 0.11 and at 0.148 AU by the TBL and the RF respectively. The next predicted orbit after planet d is at 0.29, ~ 0.36 AU.

3 Dynamical models and methods

We investigated the dynamical stability of the Gliese 581 planetary system by using numerical integrations of the

Table 2 Astrocentric, circular, non-interacting 4-planet orbital model of Vogt et al. (2012). P: orbital period, $M_{min} = m \sin i$, where i is the orbital inclination, a: semi-major axis, e: eccentricity, l: longitude of the periastron.

Planet	P	M_{min}	a	e	l
	(days)	($M_{\oplus}$)	(AU)		(deg)
e	3.15	1.84	0.028	0	138.5
b	5.37	15.98	0.04	0	338.9
c	12.93	5.4	0.073	0	175.2
d	66.71	5.25	0.22	0	235.8

planetary orbits. The model parameters were taken from the announced 4-planet and 5-planet fits of Vogt et al. (2012) and are presented in Table 2 and 3 for reference. For the mass of Gliese 581 we took $0.31 M_{\odot}$. We made the assumption of coplanarity of all orbits, and in case of the 4-planet model we checked the stability for different orbital inclinations (to the line of sight), otherwise and for the 5-planet model $\sin i = 1$ (an edge-on system) was assumed. We confined our study area to the region of the four certain and the potential fifth planet, between 0.01 and 0.41 AU. In our study, we investigated the stability of the following models:

– 5-body problem consisting of the star and the 4 certain planets (b-e) to check the long-term stability of the 4-planet system,
– restricted 6-body problem consisting of the star, 4 planets (b-e) and a massless fifth planet to search for stable regions for an additional planetary body,
– 6-body problem consisting of the star and 5 planets to verify the dynamical stability of the 5-planet system including planet g as presumed by Vogt et al. (2012).

The numerical integrations were performed using the method of Lie-integration with an adaptive step-size, which is a very fast and precise integration method due to the recurrence of the Lie-terms (Hanslmeier & Dvorak 1984; Pál & Süli 2007). In order to characterize the stability of the models, we used the Lyapunov characteristic indicator (LCI), the finite time approximation of the maximal Lyapunov Exponent, and the maximum eccentricity method (MEM). The LCI is a well known chaos indicator of a dynamical system, it estimates the exponential divergence rate of infinitesimally close trajectories in the phase space. The MEM provides information about the evolution of the orbit during the integration time through the largest value of the eccentricity of the planets and indicates close encounters and escapes from the region of motion as well.

4 Stability of the 4-planet system

4.1 Basic stability of the 4-planet model

The analysis of RV variations is able to constrain the mass (M) of exoplanets by a lower limit, since only the quantity $M \sin i$ is determined, where i is the unkown orbital inclination. Below a given value of i - or, equivalently above

given masses for the planets - we expect the system to become unstable as the dynamical interactions can increase with lower inclinations, i. e. higher planetary masses. To check for which range of inclinations the system has this basic stability, we integrated the 4-planet model (Table 2) over 1 Myr varying the inclination by $\triangle i = 5°$ from $i = 90°$ (edge on) to $i = 5°$ (almost pole on).

In all cases, the integrations show that the variations of the semi-major axes and eccentricities of the planets are not significant. The 4-planet system remains stable for 1 Myr down to $i = 5°$ (almost pole-on) and co-planar orbits. Dynamical stability with $i \geq 5°$ suggests that the mass of each planet can be ~ 12.5 times of its minimum mass. For Gliese 581 e, b, c, and d those limits are 21, 183, 62 and 60.2 $M_{\oplus}$.

In comparison, the 4-planet fit of Mayor et al. (2009) became unstable and planet e escaped from the system after a few Myrs already for $i \geq 40°$. Although their integration time was longer, the orbital parameters did not change significantly in our integration in case of smaller inclinations, which means considerably higher planetary masses and thus stronger perturbations over the time of 1 Myr. The 4-planet fit of Vogt et al. (2012) in this sense can be considered more stable.

4.2 Stability of planet e

The low mass planet e has little effect on the stability of the more massive planets in the system, but an increase in its eccentricity quickly leads to orbital crossings with planet b or ejection from the system (as it was already pointed out by Mayor et al. 2009; Vogt et al. 2012). To characterize planet e's orbit in the 4-planet model, we carried out integrations with the following grid of initial semi-major axis and eccentricity: $0.01 \leq a \leq 0.041$ AU with steps $\triangle a = 0.003$ AU and $0 \leq e \leq 1$ with steps $\triangle e = 0.01$, for a time period of $5000 P_e$, where P_e is the orbital period of planet e.

The maximum eccentricity that planet e reached over the time of the integration is plotted on the $a - e$ stability map in Fig. 1. Planet e's orbit is stable (small e_{max}, yellow color), although the vicinity around its initial $a_e = 0.028, e_e = 0$ values represents a stable island on the map, so relatively small perturbations could lead to instability and thus collision or ejection. Having varied only the eccentricity e_e, the LCI became suddenly high above $e_e = 0.22$ (data not shown). This indicates chaos, and also points to the highest eccentricity for planet e's orbit to remain stable.

We also performed integrations with different starting positions (l) for planet e varying l by $2°$ between $l = 0 - 360°$. The LCI values remain low during the time of the integration for each case (data not shown), so planet e's stability does not depend on its orbital position in the model.
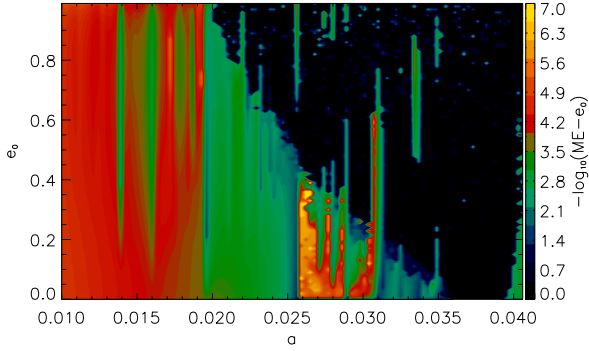
Fig. 1 a-e stability map of planet e, its maximum eccentricity is plotted as a function of semi-major axis and eccentricity (with a starting value of 0). Yellow regions are stable, black regions denote escaping orbits.
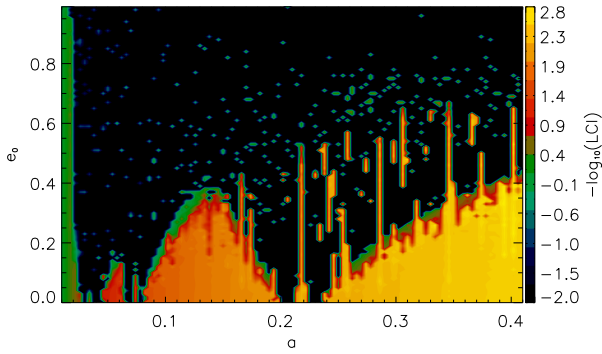

Fig. 2 LCI values of a fifth massless test planet for different initial a-e. Stable regions are marked as yellow according to the LCI.

5 Stability of the 5-planet system

5.1 Stable regions for a fifth planet

We integrated the 4-planet system with an additional massless body in order to find regions of possible orbital stability for a fifth planet. The test planet's initial parameters were varied, in one set the semi-major axis between $0.01 \leq a \leq 0.41$ AU with steps of $\triangle a = 0.001$ AU and the eccentricity $0 \leq e \leq 1$ with steps of $\triangle e = 0.01$, and in another set for the same semi-major axis range and $e = 0$, the starting position $0 \leq l \leq 360°$ with steps of $\triangle l = 2°$. The time of the integrations was 10000 P_{test} for calculating the LCI, where P_{test} is the orbital period of the test planet. The LCI values of each integration for the grid of different a, e are plotted on Fig. 2, for a, l on Fig. 3. The e_{max} that the test planet reached over 5000 P_{test} was calculated for the same grid of a, e, and for 8 different starting orbital positions with steps $\triangle l = 45°$ between $l = 0 - 315°$. The average of these 8 e_{max} values are represented on one map on Fig. 4.

The orbits of a fifth fictitious planet are chaotic close to the innermost planets e and b, but extensive stable regions exist between the larger planets c and d, and outside planet
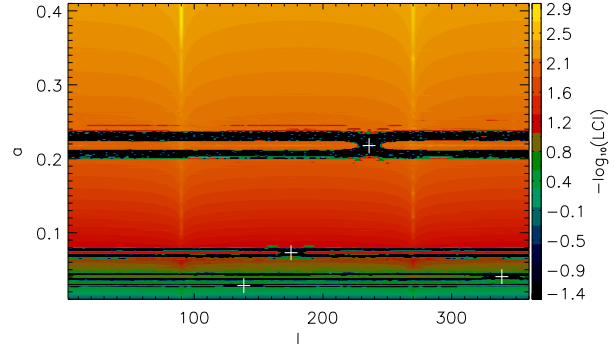

Fig. 3 LCI values of a fifth massless test planet for different initial semi-major axis (a) and starting position (l). Chaotic orbits are marked with colors towards black, stable orbits towards yellow.
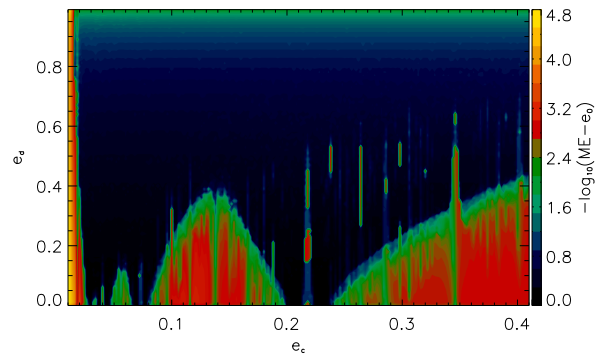

Fig. 4 Maximum eccentricity of a fifth massless test planet. Each a, e point on the map represents an average of the maximum eccentricities that the test planet reached over the time of the integrations started from 8 different starting positions in the model.

d, with relatively low eccentricities (Fig. 2). The starting position of the fictitious planet only plays a role in its stability around the innermost planets and the orbit seems less chaotic in the outer part of the system (Fig. 3). The $a-e$ stability map with the maximum eccentricity essentially shows the same boundaries for stable regions, in fact the average e_{max} values confirm that irrespective of the starting position of the test planet, its orbit will be stable in the region between the super-Earth planets and beyond them (Fig. 4).

There are small stable islands at the distance of planet d ($a = 0.22$ AU), where both the e_{max} and the LCI have low values at the end of the integration (Fig. 3. and Fig. 4). This points to the possibility of Trojan planets orbiting the star in 1:1 mean motion resonance with planet d.

According to these stability maps, the additional planets, predicted by the TBL and RF between planet c and d at 0.11 and 0.15 AU, and beyond planet d at 0.29 and 0.36 AU, would have stable orbits with low eccentricities.

Table 3 Astrocentric, circular, non-interacting 5-planet orbital model of Vogt et al. (2012). P: orbital period, $M_{min} = m \sin i$, where i is the orbital inclination, a: semimajor axis, e: eccentricity, l: longitude of the periastron.

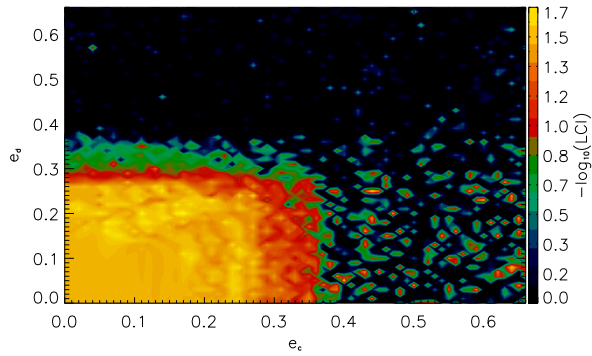| Planet	P (days)	M_{min} $(M_\oplus)$	a (AU)	e	l (deg)
e	3.15	1.86	0.028	0	141.9
b	5.37	16.0	0.04	0	338.4
c	12.93	5.3	0.073	0	181.0
g	32.13	2.24	0.13	0	55.3
d	66.67	5.94	0.22	0	227.3

Fig. 5 LCI values of the orbit of planet g as a function of eccentricity of the adjacent planets c and d. The yellow to red rectangular region indicates stable orbits, initial points in the dark regions result in chaotic motion.

5.2 Stability of planet g

The 5-planet model of Vogt et al. (2012) (as a reference see Table 3) was integrated for 1 Myr to verify its long-term stability. All 5 planets remained stable during the long integration time and their orbital parameters did not change significantly, so this 5-planet solution of the RV data can be considered dynamically stable.

If planet g exists, it is a 2.2 $M_\oplus$ planet orbiting between two super-Earth sized planets in the middle of the star's classical liquid water habitable zone. To further characterize the stability of the orbit of this possibly rocky and habitable planet, we ran two more set of integrations. In one set, for a time of 5000 P_g, the eccentricity of the adjacent planets c and d were varied until the point when their orbits cross each other. According to the LCI of planet g on Fig. 5., planet g's orbit is not chaotic and thus can be considered stable in cases where the eccentricity of planet c stays below $e_c \leq 0.32$ and for planet d $e_d \leq 0.28$.

Since the true orbital period and therefore semi-major axis of planet g is still uncertain, as well as planet d's real eccentricity could be greater than zero, in another set of integrations, also for a time of 5000 P_g, we varied a_g in the range between the neighbouring planets and e_d until it would cross the orbit of planet c. Not surprisingly, as Fig. 6. shows, the more elliptic the orbit of planet d, the further away planet g has to be from it in order to remain stable. At
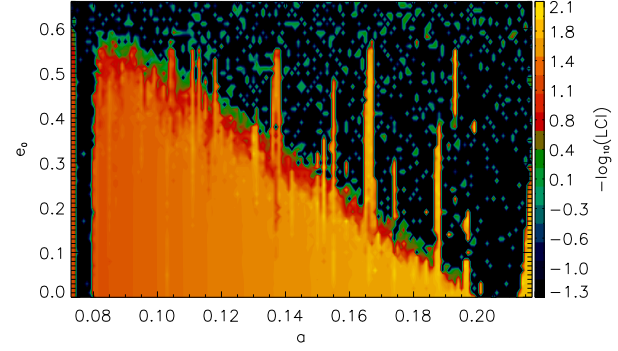

Fig. 6 Stability of planet g as a function of planet d's eccentricity and the semi-major axis. Yellow marks the stable, black end of the color bar the chaotic orbits according to the LCI.

the largest distance, planet g's orbit would be still stable in case of $e_d \approx 0.55$.

6 The problem of orbital eccentricity

In the process of fitting multi-planet models to precise RV data, it is a question of choice whether to allow the orbital eccentricities to float freely or to hold them fixed at zero. As the case of the Gliese 581 planetary system shows, freely floating eccentricities can lead to solutions that are unstable and therefore unphysical despite providing good fits to the RV data. On the other hand, forced circular orbits might be too strong a restriction.

In the previous section we derived limits for the eccentricity of planets c and d with planet g in the system, now we will investigate the situation of the inner planets. We have assumed that given its higher mass planet b is likely to be more stable in comparison to the adjacent planets, therefore we looked at the stability of planet e for a range of intial e_e and e_b, and the stability of planet c for a range of initial e_b and e_c (in this case planet e was left out of the system). The maximum eccentricity was calculated in both cases over a time period of 5000 P_e and 5000 P_c, respectively. The eccentricities ranged until the elliptical orbit of one planet crossed the other one's circular orbit.

The maximum eccentricity on Fig. 7. indicates that planet e's stability is ensured when the adjacent planet b's eccentricity stays relatively low, $e_b \leq 0.075$, and its own orbital eccentricity below $e_e \leq 0.2$, approximately the same upper limit as the one based on the LCI. Small stable regions exist with eccentricities above $e_e = 0.3$ too, though these isolated configurations seem less likely to remain stable for a longer time. Looking at the stability of planet c as a function of e_b and e_c (Fig. 8.), it is apparent that planet c puts less constraint on the eccentricity of planet b (which is then mainly given by the smaller planet e). While in case of circular or near-circular orbits, the upper limit of planet b's eccentricity is $e_c \leq 0.32$.
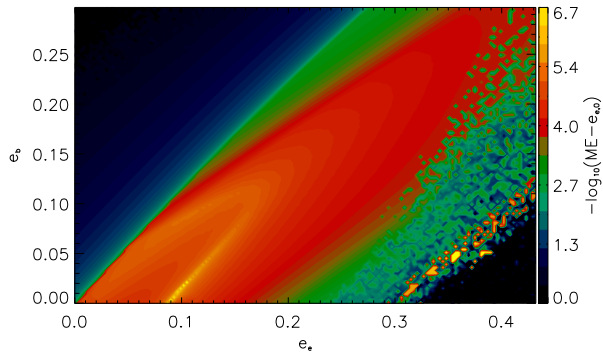
Fig. 7 Stability of planet e is characterized with its the maximum eccentricity as a function of e_e and e_b. Black denotes unstable, whereas yellow stable configurations.
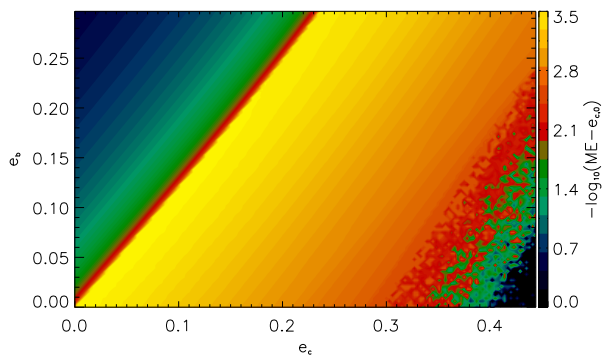

Fig. 8 Stability of planet c is characterized with its the maximum eccentricity as a function of e_b and e_c. Black denotes unstable, whereas yellow stable configurations.

7 Conclusions

The long-term numerical integrations show that the latest 4-planet all-circular model of the Gliese 581 exoplanetary system presented by Vogt et al. (2012) is dynamically stable for 1 Myr. The innermost planet e, which was found to be sensitive to small perturbations due to its low mass and the tight packing of the inner planets, remains stable, however the stable region on the a-e plane around it is rather small and its eccentricity cannot be larger than 0.2.

A fifth planetary body in the 4-planet system could have a stable orbit between the two super-Earth planets c and d, and there is an extensive stable region for an additional planet beyond the orbit of planet d. The Titius-Bode law and Ragnarsson's formula applied to the Gliese 581 planetary system both predict planets at distances from the star, where large stable regions exist.

The 5-planet model of Vogt et al. (2012) including planet g is also dynamically stable on a longer timescale. The existence of planet g is fully supported from the dynamical point of view. In fact a low-mass planet like planet g can be considered stable for a wider range of orbital configurations in the region between the two super-Earth planets.

Modelling the system in order to find a good fit to the RV curve was found to be quite complex, especially in regards to the question of how they treat the eccentrities of the orbits. The eccentric Keplerian model of Forveille et al. (2011) was very unstable, and while the models of Vogt et al. (2012) with initial circular orbits are dynamically stable over a longer time period, the true orbits might be elliptic as a consequence of dynamical interactions between the planets. Our simulations put dynamical constraints on the eccentricity of the planets, and these limits can in turn be used to help find the best stable model to fit the RV measurements.

References

Anglada-Escude, G., López-Morales, M., Chambers, J. E.: 2010, ApJ 709, 168-178

Anglada-Escude, G., Dawson, R. I.: 2010 ApJL, submitted; arXiv:1011.0186v2 [astro-ph.EP]

Bonfils, X., Forveille, T., Delfosse, X., et al.: 2005, A&A 443, 15-18

Cuntz, M.: 2012, PASJ 64, 73

Hanslmeier, A., Dvorak, R.: 1984, A&A 132, 203-207

Forveille, T., Bonfils, X., Delfosse, X., et al.: 2011, A&A, submitted; arXiv:1109.2505v1 [astro-ph.EP]

Gregory, P. C.: 2011, MNRAS 415, 2523-2545

Mayor, M., Bonfils, X., Forveille, T., et al.: 2009, A&A 507, 487-494

Pál, A., Süli, Á.: 2007, MNRAS 381, 1515-1526

Poveda, A., Lara, P.: 2008, RMxAA 44, 243-246

Ragnarsson, S-I.: 1995, A&A 301, 609-612

Selsis, F., Kasting, J. F., Levrard, B., Paillet, J., Ribas, I., Delfosse, X.: 2007, A&A 476, 1373-1387

Tadeu dos Santos, M., Silva, G. G., Ferraz-Mello, S., Mtchtchenko, T. A.: 2012, CeMDA 113, 49-62

Tuomi, M.: 2011, A&A 528, L5

Udry, S., Bonfils, X., Delfosse, X., et al.: 2007, A&A 469, 43-47

Vogt, S. S., Butler, R. P., Rivera, E. J., Haghighipour, N., Henry, G. W., and Williamson, M. H.: 2010, ApJ 723, 954-965

Vogt, S. S., Butler, R. P., Haghighipour, N.: 2012, AN 333, 561-575